Proceedings of the ASME 2025 44th International Conference on Ocean, Offshore and Arctic Engineering
OMAE2025
June 22-27, 2025, Vancouver, British Columbia, Canada

OMAE2025-156801

DESIGN AND OPTIMIZATION OF A HYBRID ENERGY SYSTEM FOR AN ICE-CLASS RESEARCH VESSEL

Dheeraj Gosala[1,*], Tobias Lampe[1], Gesa Ziemer[1], Sören Ehlers[1]

[1]German Aerospace Center (DLR) - Institute of Maritime Energy Systems, Geesthacht, Germany

ABSTRACT

Hybrid energy systems are investigated as a viable alternative to conventional energy systems typically consisting of multiple diesel engines, on ice class vessels. Vessels bearing ice class notation experience significant disparities in load profiles between typical voyages and those involving occasional icy conditions. Ice class rules mandate considerably higher installed power than necessary for regular service, which can reduce the average operating efficiency of a conventional energy system. This paper demonstrates the performance of a 50-meter research vessel operating mainly in the Baltic Sea with ice class 1A. Ship resistance is calculated in open water and ice, characteristic time-based load profiles are generated for a selected route over three voyage conditions, and various hybrid energy system configurations are analyzed. The peak propulsion loads even in mild winter conditions with ice are observed to be over 4 times as high as open water operation in summer. Results indicate that modularizing the energy system with multiple gensets results in 6.9%, 7.8% and 13.8% energy savings over the three voyages. While battery hybridization does not show outright fuel savings over most voyages, it compensates for non-optimal modularity of the gensets over specific voyages by yielding up to 1.8% fuel savings and enables optimal energy system operation over a wider range of voyages. Finally, it is determined that an ice class certified energy system performs just as efficiently as a comparable downsized energy system, if the genset installation is appropriately modularized.

Keywords: Ice Class Vessel, Ice Load Modelling, Hybrid Energy System, Diesel Gensets, Battery

1. INTRODUCTION

Shipping contributes to almost 80% of the global trade today. While most of the maritime transport occurs in open waters, there is increasing interest in shipping through seas with ice cover, enabling not only greater accessibility to Arctic regions, but also shorter distances between Europe and Asia through the Northern Sea Route (NSR). In addition to greater international commerce, ice-class vessels also contribute to scientific research and exploration efforts amidst some of Earth's most challenging environments. Almost 133,000 trips were made in the Arctic region each year on average between 2015-2017 by over 5500 different vessels [1] analyzed 400,000 vessel transits in the Arctic region between 2015 and 2017.

Ice class vessels need to be specially designed for operation under various ice conditions, including strengthened hull, greater installed power onboard, and additional redundancy. Heikkilä et al. [2] analyzed the EU Monitoring, Reporting and Verification (MRV) database and statistically concluded that ice classed ships had on average 11% more hull mass, 13% more main engine power and 13% less dead weight capacity than ships without ice class. Furthermore, ice classification showed lower fuel consumption for three vessel types (bulk carrier, chemical tanker, and ro-pax vessel), higher fuel consumption two vessel types (general cargo ship and ro-ro vessel) and an unclear effect in container ships and oil tankers. Braithwaite and Khan [3] analyzed the various vessel design aspects that need to be addressed to enable an offshore patrol vessel to operate in ice conditions, and concluded that conforming to ice class 1C and 1AS resulted in 732 kW and 1262 kW higher electrical load, 9 t and 11.7 t additional weight, and 8% and 18% higher cost, respectively. Solakivi et al. [4] concluded that Polar Class compliant vessels can consume up to 50% more fuel and carry 20% less cargo than vessels without an ice class due to additional engine power and increased hull weight.

Vessels bearing ice class notation undergo significant disparities in load profiles between typical voyages and those involving occasional icy conditions. Modern ice class vessels typically consist of a diesel-electric propulsion system, and hybridizing the energy system with batteries can enhance overall efficiency. Wang et al. [5] explored and optimized a diesel engine/battery/shore power propulsive system for a mini polar cruise vessel and achieved 0.27% fuel reduction and 37.48% increase in annual pure electric time with a 7.85% lifecycle cost over a conventional diesel electric propulsive system. Zhou et al. [6, 7] showed that a hy-

*Corresponding author: dheeraj.gosala@dlr.de
Documentation for `asmeconf.cls`: Version 1.38, March 21, 2025.

brid system on the Swedish icebreaker 'ENVIK' yielded up to 22.4% fuel savings over a diesel-electric propulsion system under ice-loading conditions, and 39.5% fuel savings under open water conditions. Hanninen et al. [8, 9] showed that battery hybridization can improve the overall power efficiency over diesel- as well as LNG-based propulsion systems for the Finnish icebreaker 'Polaris', based on a three-propulsion unit concept based on ABB Azipods. Fengxiang et al. [10] proposed a diesel/battery hybrid electric propulsion system (HEPS) for a polar icebreaker and achieved 2.78% less fuel consumption and 29.07% cost saving. Zhu et al. [11] demonstrated that a hybrid electric propulsion system can result in 10% improvement in fuel consumption, GHG emissions and net present value (NPV) on an anchor handling tug supply vessel.

Designing the optimal energy system requires careful consideration of ship load profiles that vary across different routes and environmental conditions, and the vessel's power consumption needs to be modelled at reasonable speeds in different ice conditions [12]. Kondratenko et al. [13] presented a framework for holistic multi-objective optimization of Arctic offshore supply vessels (OSVs) for cost- and eco-efficiency, and concluded that the overall best performing vessels have a moderate ice class and ice-breaking capabilities. However, this analysis did not consider the impact of wind- and wave- parameters in open water and ice. Kondratenko et al. [13] also presented a decision support framework for holistic and sustainable design and optimization of Arctic ships for different cold regions and purposes of operation, and applied it to battery-driven Arctic offshore wind farm service and offshore support vessels. Palmen et al. [14] concluded that marine diesel oil (MDO) is the most convenient solution for an ice-breaking Arctic research ship with electrical propulsion system, based on constraints around space, operational range, and endurance. However, liquefied natural gas (LNG) and methanol can yield 25% and 9% life cycle cost reductions with 24% and 13% CO_2 emission reductions, respectively, if the ship's arrangement were radically redesigned. However, the fuel consumption of the various energy system concepts were not analysed over the operating profiles.

While previous research showed the benefits of battery hybridization of the energy system, and presented design methodologies for selecting an appropriate fuel and energy converter, the energy system configuration is assumed to be fixed. The impact of different energy system parameters such as number of gensets installed, battery capacity, etc. have not been previously considered. Further, the impact of ice class notation on energy system performance and fuel consumption has not been analyzed in detail over specific routes and voyage conditions.

1.1 Scope of this work

This paper presents the impact of Ice Class Notation 1A on the optimal energy system design and operation of a research vessel, as well as the resulting benefits of battery hybridization of the energy system. The impact of various energy system design parameters on the overall energy efficiency is demonstrated. A case study featuring a 50-meter research vessel operating mainly in the Baltic Sea is presented to demonstrate these findings.

The paper is structured as follows: Section 2 presents the methodology followed in this work involving modelling propulsion loads of the vessel in the presence of ice in water as well as without ice, route simulation, ice class requirements, and onboard energy system analysis. The vessel, corresponding ice-class requirements, route, and voyages considered in the case study are presented in Section 3. Section 4 presents the results obtained over the case study, including the propulsion and total load profiles, and impact of various energy system design parameters on overall energy efficiency. Finally, Section 5 summarizes the key findings and takeaways of this work.

2. METHODOLOGY

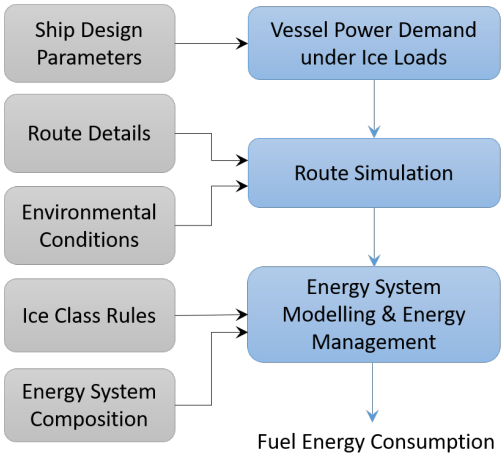

FIGURE 1: METHODOLOGY FOR ICE CLASS VESSEL ENERGY SYSTEM DESIGN AND ANALYSIS

The methodology followed in this paper is described in Figure 1, and is derived from a holistic in-house vessel- and energy system- modelling framework [15]. Firstly, the vessel power demand is calculated for a defined vessel, across a range of environmental conditions including open water, broken ice, and level ice using the approaches presented in Sections 2.1. This requires the ship design parameters as an input, which are defined for the case study in Section 3.

Next, a route simulation is performed over the selected route and environmental conditions to obtain a time- and distance-based power demand profile as elaborated in Section 2.2. A constant route is chosen in this study, however under different environmental conditions, resulting in multiple power demand profiles.

Lastly, reduced-order models of various onboard energy system components are developed, and an optimization-based energy management algorithm [16] is used to enable optimal operation of the hybrid energy system over the developed load profile(s), as described in Section 2.3. The optimal fuel consumption is ascertained from this algorithm, and is the final output of this methodology. The ice class rules are analyzed to establish the installed power onboard. The fuel energy consumption is calculated and analyzed across various combinations of energy system component sizes.

2.1 Vessel Power Demand Calculation

The thrust T needed to propel a vessel is calculated by Equation 1

$$T(1-t) = R_{CW} + R_{AW} + R_W + R_I. \tag{1}$$

where t is the thrust deduction factor, R_{CW} is the calm water resistance, R_{AW} is the added wave resistance, R_W is the wind resistance, and R_I is the ice resistance, all of which are described below.

The calm water resistance R_{CW} is derived using the Holtrop & Mennen method [17]. The added wave resistance R_{AW} is derived using the method provided by Kim et al [17], as shown in Equation 2. The wave resistance due to regular waves is split into contributions from wave reflection (diffraction) and ship motion (radiation), taking into account significant wave height, wave period, wave angle of attack as well as several vessel related parameters, such as block coefficient and bow opening angle. The added resistance in irregular waves is calculated based on the assumption that the irregular seaway is composed of a superposition of regular waves of different frequency and direction.

$$R_{AW} = 2\int_{-\pi/2}^{\pi/2}\int_{0}^{\infty}\frac{R_{AW,reg}(\omega,\alpha,v_S)E(\omega,\alpha)}{\zeta^2}d\omega d\alpha, \tag{2}$$

$$E(\omega,\alpha) = S(\omega)D(\alpha). \tag{3}$$

where ω is the wave frequency, α is the angle of attack, and ζ is the wave amplitude. E is the directional wave spectrum, which is composed of the standard frequency spectrum S based on the JONSWAP spectrum [18], and a cosine-power based angular distribution function D [19]. Wave peakedness as well as spreading factor of the natural seaway are taken into account.

The wind resistance R_W is derived using the method provided by Blendermann [20] using the set of coefficients for ship type 'research ship'. The ice resistance R_I depends on the interaction between the ice and the hull, which is dictated by the hull shape and the physical parameters of the surrounding ice and its condition, i.e. broken or solid ice. The applicable model to calculate the corresponding additional resistance needs to be chosen on a case-by-case basis and is further described in Section 3. No wave resistance is considered for level ice conditions, while standard wave conditions are used for computing wave resistance in broken ice. The interaction between ice resistance and the waves are not considered in this study, and are out of the scope of this paper.

The thrust deduction factor t models the interplay between the propeller and hull, and is set constant at 0.07.

To account for the propeller, the characteristic curves of thrust coefficient, torque coefficient and efficiency are modelled as third-order polynomials based on open water data from commercially available products from propeller designers. Given required thrust and propeller inflow speed, the equations are solved for their zero points to deliver the necessary rotational speed. The propeller inflow speed is obtained using a generic value of 0.85 for the wake fraction. The torque is calculated directly from the characteristic curves based on the rotation rate of the propeller, yielding Equation 4 for the power calculation

$$P = 2\pi Q n. \tag{4}$$

2.2 Route Simulation

The ice conditions for a typical, mild winter in the Baltic sea are derived from the open-access Copernicus dataset [21], which provides information on ice thickness and concentration at high spatial resolutions. The values are derived from fit Weibull distributions using the charts from 2018 to 2023. The selected routes are first discretized and Equations 1- 4 are applied at each discrete location by utilizing the weather and ice data at that location, at an appropriate time instant, to obtain the propulsion load profiles.

2.3 Energy System Analysis

The research vessel has an all-electric energy system, wherein the diesel gensets and battery are electrically connected to a main distribution grid. The propulsion system and bow thrusters are driven by electrical motors, which draw electrical power from the main distribution grid. Similarly, the electrical power required for all hotelling loads is also drawn from the main distribution grid. The centralized electrical grid architecture enables optimal power sharing between various onboard power sources to meet a total electrical load demand from all onboard consumers.

2.3.1 Diesel Genset Modelling. Figure 2 presents the energy efficiency of a diesel genset as a function of the normalized output electrical power. The genset efficiency monotonically increases with increasing load, achieving peak efficiency at rated power. The correlation between diesel power consumption of a single genset P_{dsli}, its output electrical power P_{gi}, and efficiency η_g is modelled by a quadratic function as shown in Equation 5a [16]. The quadratic curve is fit for the points shown in Figure 2 and extrapolated to determine fuel consumption at zero electrical power. All active diesel gensets are considered to operate with equal load sharing among them to minimize fuel consumption. The total diesel power consumption by N_g gensets P_{dsl} and is shown in Equation 5b.

$$\begin{aligned} P_{dsli} &= \alpha_2 P_{gi}^2 + \alpha_1 P_{gi} + \alpha_0 \\ \eta_g &= \frac{P_{gi}}{P_{dsli}} \end{aligned} \tag{5a}$$

$$\begin{aligned} P_{dsl} &= N_g P_{dsli} \\ 0 \le N_g &\le N_g^{max} \end{aligned} \tag{5b}$$

2.3.2 Battery Modelling. Battery systems experience an energy loss between the electrical power at the terminals and the charge stored in the battery. Figure 3 presents the correlation between the energy losses of a battery system P_b^{loss} and the electrical power output. A negative power output for the battery indicates battery charging, while positive power refers to battery discharging. The losses of the battery system vary nearly parabolically with charging or discharging power, and are therefore modelled

quadratically as shown in Equation 6a [16, 22]. The correlation between the change in battery energy E_b, battery power P_b, and state of charge SOC_b are shown in Equation 6b.

$$P_b^{loss} = \kappa P_b^2 \tag{6a}$$

$$\begin{aligned} \frac{dE_b}{dt} &= -P_b - \kappa P_b^2 \\ SOC_b &= \frac{E_b}{E_b^{max}} \end{aligned} \tag{6b}$$

where E_b^{max} is the energy capacity of the battery

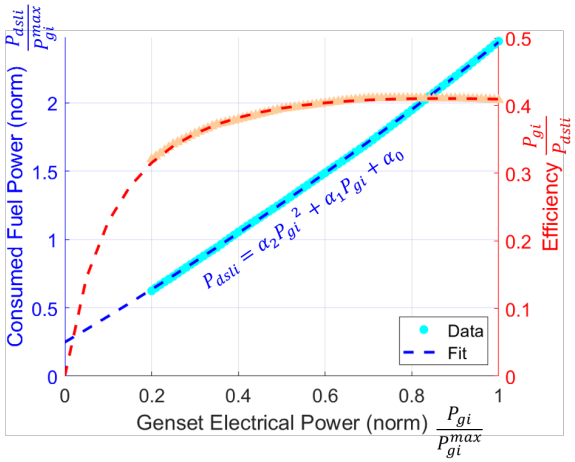

FIGURE 2: EFFICIENCY OF A DIESEL GENSET AS A FUNCTION OF OUTPUT ELECTRICAL POWER

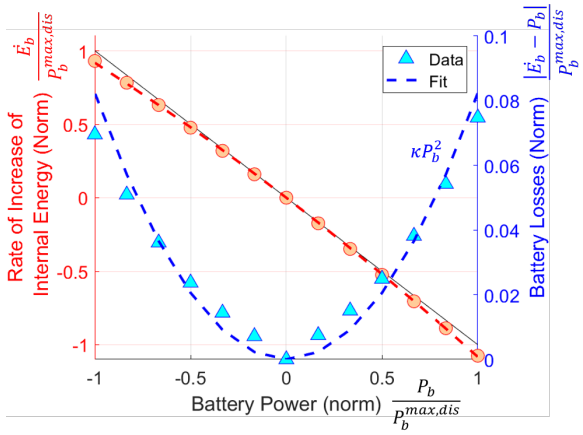

FIGURE 3: BATTERY LOSSES AS A FUNCTION OF OUTPUT BATTERY POWER

2.3.3 Optimization-based energy management. The overall power demand is met by a combination of onboard power sources including multiple gensets and a battery system. The power demand is optimally split among multiple energy converters by minimizing the total energy consumption over the load profile, using Dynamic Programming (DP), as presented by the authors in [16]. The DP algorithm aims at determining the optimal sequence of battery power $P_{b,k:1..N}$ over the load profile steps $P_{dmd,k:1..N}$, to minimize the overall fuel energy consumption J, as shown in Equation 7. The various constraints for this optimization are defined by Equations 8a- 8e.

$$J = \sum_{k=1}^{N} \left(\left(\alpha_2 {P_{gi,k}}^2 + \alpha_1 P_{gi,k} + \alpha_0 \right) N_{g,k} \right) \Delta t \tag{7}$$

$$P_{dmd,k} = P_{gi,k} N_{g,k} + P_{b,k} \tag{8a}$$

$$E_{b,k+1} = E_{b,k} - \Delta t \left[P_{b,k} + \kappa P_{b,k}^2 \right] \tag{8b}$$

$$\begin{aligned} 0 \le P_{gi,k} &\le P_{gi}^{max} \\ P_b^{max,chg} \le P_{b,k} &\le P_b^{max,dischg} \\ SOC_b^{min} \le SOC_{b,k} &\le SOC_b^{max} \end{aligned} \tag{8c}$$

$$SOC_{b,N} \ge SOC_{b,1} \tag{8d}$$

$$\mathcal{R}_g + \mathcal{R}_b \ge \mathcal{R}^{thd} = \Lambda P_g^{max} \tag{8e}$$

The total power delivered by the power system comprises of the power P_{gi} delivered by each of N_g active gensets, and P_b delivered by the battery system at each time step k, as shown by Equation 8a. The evolution of the battery state of charge SOC_b, defined by Equation 6b, is used in discrete form to define the state evolution, as shown in Equation 8b. The power produced by individual gensets and the battery lie within their respective power and energy limits, as shown in Equation 8c. The battery is operated in a 'charge sustaining' mode, wherein the battery SOC at the end of the voyage is at least the same as that at the start of the voyage, as shown by Equation 8d. Finally, the energy system is operated with a minimum power reserve $\mathcal{R}^{thd}$ at all times of the voyage, which is proportional to the total installed power of the vessel with a factor Λ, as shown in Equation 8e.

DP is implemented by discretising the battery SOC (state) in 601 steps, and the battery power (control variable) in 501 steps. For a given battery SOC, the 'cost-to-go' function $J_{c2g,k}$ at any time instant k is defined as the fuel energy consumption at that time step, as defined by Equation 9. The 'value function' $\mathcal{V}_k$ at the time step k is the minimum sum of the cost-to-go function $J_{c2g,k}$ at that time step k and the value function $\mathcal{V}_{k+1}$ at the next time step $(k+1)$, as shown by Equation 10. The value function at the final time step $\mathcal{V}_N$ is defined to be 0 when constraint 8d is respected. The value function at all time steps and battery SOC is set to infinity when any of the constraints 8a- 8e are violated. The value function represents the minimum fuel energy that will be consumed from that time step and battery SOC to reach the end of the load profile while respecting all constraints.

$$J_{c2g,k} = \left(\alpha_2 P_{gi,k}^2 + \alpha_1 P_{gi,k} + \alpha_0 \right) N_{g,k} \tag{9}$$

$$\mathcal{V}_k = \begin{cases} \min\left(J_{c2g,k} + \mathcal{V}_{k+1}\right) & ;\text{constraints 8a- 8e respected} \\ \text{inf} & ;\text{otherwise} \end{cases}$$

$$\mathcal{V}_N = \begin{cases} 0 & ; SOC_{b,N} \geq SOC_{b,1} \\ \text{inf} & ;\text{otherwise} \end{cases} \quad (10)$$

The optimal battery power P_b^* at each time step and battery SOC is calculated by minimizing the value function at that time step. The calculation of the cost-to-go function and optimal battery power is first done backwards from the last time step to the first step starting from the final value $\mathcal{V}_N$, and a map of optimal battery powers at each time step, at all possible battery SOC, is created. The load profile is subsequently simulated, starting from a defined initial condition ($E_{b,1}$), by applying the pre-determined optimal action $P_{b,k}^*$ at each step $k = 1...N$ based on instantaneous battery SOC.

3. CASE STUDY

3.1 Vessel Parameters

A case study is performed on a research vessel being conceptualized by DLR, with ice class 1A according to Finnish-Swedish ice class rules. The vessel will primarily serve to investigate new energy system concepts under real-world operating conditions, across various environmental conditions, predominantly in the North and Baltic seas. The vessel will majorly operate in open water, and will experience significantly lower power demands in comparison to the installed power as stipulated by the rules. The vessel will sail occasionally in icy conditions to validate novel energy system concepts under highly time-varying load profiles, as well as demonstrate the energy system concepts within cold surroundings. While the vessel can break thin level ice occasionally, it is not designed for ice breaking and will not be able to operate in icy conditions during severe winters. The various ship design parameters of the research vessel are presented in Table 1.

Figure 4 shows the calm water resistance of the vessel, comparing model test results extrapolated to full scale with that obtained by the Holtrop & Mennen method [17], which is used in Equation 1. The resistance, thrust, and power of the vessel at design speed is shown in Table 2.

3.2 Ice Class Rules and Installed Power

The installed power needs to fulfill the minimum power requirement per the Swedish-Finnish ice class rules [23], which can be calculated based on the geometry of the vessel. The rules stipulate a minimum engine output for new ships as described by Equation 11.

$$P = \frac{K_e}{D_P}\left(\frac{R_{CH}}{1000}\right)^{1.5}$$
$$R_{CH} = C_3 C_\mu \left(H_F + H_M\right)^2 \left(B + C_\psi H_F\right) + C_4 L_{PAR} H_F^2 + C_5 \left(\frac{LT_{IWL}}{B^2}\right)^3 \frac{A_{wf}}{L} \quad (11)$$

where R_{CH} is the resistance of the ship in a channel with brash ice without consolidated layer.

TABLE 1: RESEARCH VESSEL PARAMETERS

Parameter	Variable	Unit	Value
Design Speed		kn	10
Speed in Ice		kn	3
Length between Perpendiculars	L	m	48
Beam	B	m	11
Draught	T	m	3.2
Displacement		m^3	995.5
Stem Angle	ϕ	deg	22.5
Waterline Entrance Angle	α	deg	44.7
Ice-Hull Friction Coefficient	μ	-	0.1
Upper ice water line	T_{IWL}	m	3.3
Length of the parallel midship body	L_{PAR}	m	11.824
Area of waterline at the bow	A_{wf}	m^2	151.25
Waterline angle at B/4	$\alpha_{B/4}$	deg	19.3
Rake of the stem at centerline	ϕ_1	deg	90
Rake of the bow at B/4	ϕ_2	deg	41.4

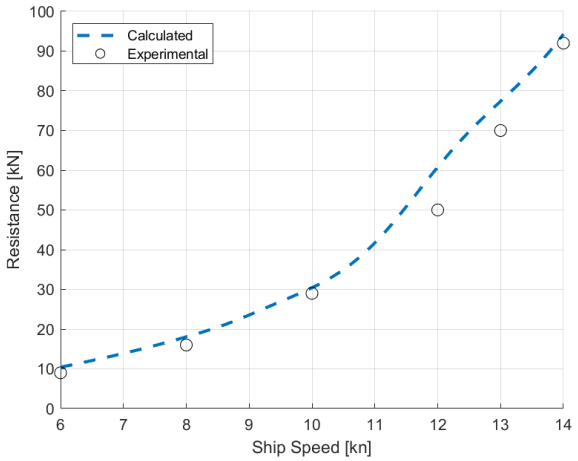

FIGURE 4: CALM WATER RESISTANCE

The equations defined in Equation 11, vessel parameters in Table 1, and constants defined in Equation 12 are used to define the minimum required installed power to meet the ice class rules. The constant K_e is set at 1.44 corresponding to two electric rudder propellers. The minimum value of the term $\left(\frac{LT}{B^2}\right)^3$ is 5, and therefore assumed to be 5 for this case. T_{IWL} refers to the upper or lower actual ice waterline corresponding to the higher load. In this case, the upper ice water line creates a higher load, and therefore $T_{IWL} = 3.3m$. Accordingly, the resistance in brash ice is calculated to be 142 kN. The minimum required installed power for propulsion is therefore calculated to be 1112 kW.

TABLE 2: RESISTANCE, THRUST AND POWER DEMAND AT DESIGN SPEED

Parameter	Calculated	Experimental	Error [%]
Resistance [kN]	31.9	33	3.2
Thrust [kN]	34.3	35.7	3.9
Power [kW]	224	234	4.27

TABLE 3: ROUTE INFORMATION

Average Travel Time	165 h
Route Type	Round Trip
Start Harbor	Kiel
End Harbor	Lulea

$$
\begin{aligned}
K_e &= 1.44 \\
\left(\frac{LT}{B^2}\right)^3 &= 5 \\
T_{IWL} &= 3.3 \\
C_\psi &= 0.047 \cdot \psi - 2.115 \\
H_F &= 0.26 + (H_M B)^{0.5} \\
H_M &= 1.0 \text{ for ice class 1A} \\
C_\mu &= 0.45, C_3 = 845, C_4 = 42, C_5 = 825 \\
\psi &= \arctan\left(\frac{\tan\phi_2}{\sin\alpha_{B/4}}\right)
\end{aligned}
\tag{12}
$$

The hotel loads are assumed to be as high as 300 kW. Therefore, the installed power in this case study is assumed to be 1500 kW to satisfy the ice class rules and the assumed hotel loads, with a safety margin.

3.3 Ice Resistance

Various models are available in literature to calculate the ice resistance R_I in different ice conditions. An ice class vessel with 1A typically follows broken channels generated by ice breakers. This leads to deviations of the route from the ideal track. The thickness of the ice inside these channels is not straightforwardly accessible by e.g. satellite data. Furthermore, the resistance may vary significantly based on the actual and local channel conditions. For a consistent and simplified approach, this case study is conducted under the assumption that the ship follows its intended track regardless of ice conditions, and operates either in broken ice or in level ice condition instead of broken channels. If the required power exceeds the installed power defined by the ice class rules, the vessel slows down, while maintaining a speed not lower than 3 kn to prevent getting stuck in the ice. This approach aids to consistently calculate an ice resistance based on parameters obtained from satellite data for a given route, which provides sufficiently realistic order of magnitude for required power in icy waters for the vessel at hand for the purpose of demonstrating the energy system optimization methodology.

State-of-the art methods with low computational effort are used to calculate the ice resistance R_I. The Lindqvist approach [24] is used for level ice conditions when ice concentration is 100%, and the Colbourne approach [25] is used for broken ice conditions, as described below.

Level ice conditions The Lindqvist approach [24] is used to calculate the ice resistance under level ice conditions, wherein the total ice resistance comprises of breaking resistance R_B, crushing resistance R_C, and submersion resistance R_S, as shown in Equation 13. The breaking, crushing, and submersion resistances are calculated using Equations 14, 15 and 16, respectively.

$$
R_I = (R_C + R_B)\left(\frac{1 + 1.4 v_S}{\sqrt{g h_I}}\right) + R_S\left(\frac{1 + 9.4 v_S}{\sqrt{g L}}\right) \tag{13}
$$

where v_S is the ship velocity, g is the acceleration due to gravity, h_I is the ice thickness, and L is the ship length between perpendiculars.

$$
\begin{aligned}
R_B = \frac{27}{64}\sigma_f B \frac{h_I^{1.5}}{\sqrt{\frac{E}{12(1-\nu^2)\rho_W g}}}\Bigg(\tan(\psi) \\
+ \mu\frac{cos(\phi)}{cos(\psi)\sin(\alpha)}\Bigg)\left(1 + \frac{1}{cos(\psi)}\right)
\end{aligned}
\tag{14}
$$

$$
R_C = 0.5\sigma_f h_I^2\left(\tan(\phi) + \mu\frac{cos(\phi)}{\cos(\psi)}\right)\Bigg/\left(1 - \mu\frac{\sin(\phi)}{\cos(\psi)}\right) \tag{15}
$$

$$
\begin{aligned}
R_S = \rho_g g h_{ice} B\Bigg(\frac{T(B+T)}{B+2T} + \mu\Bigg(0.7L - \frac{T}{\tan(\phi)} - \frac{B}{4\tan(\alpha)} \\
+ T\cos(\phi)\cos(\psi)\sqrt{\frac{1}{\sin(\phi)^2} + \frac{1}{\tan(\alpha)^2}}\Bigg)\Bigg)
\end{aligned}
\tag{16}
$$

where σ_f is the flexural strength, ν is the Poissons ratio, ρ_W is the density of water, ρ_g the density difference between ice and water, μ is the friction coefficient between ship hull and ice, B is the ship breadth, T is the ship draught, ψ is the normal angle, ϕ is the stem angle, and α is the waterline entrance angle. The normal angle ψ is calculated from the waterline entrance angle α and the stem angle ϕ as shown in Equation 17.

$$
\psi = \arctan\left(\frac{\tan(\phi)}{\sin(\alpha)}\right) \tag{17}
$$

Broken ice conditions The ice loads under broken ice conditions are calculated using the Colbourne approach detailed in Xue et al [25]. The approach is mathematically described by Equations 18- 20.

$$
R_I = \frac{1}{2} C_p \rho_I B h_I v_S^2 \eta^n \tag{18}
$$

$$
C_p = k_c Fr_I^{-k_b} \tag{19}
$$

TABLE 4: ICE PARAMETERS

Parameter	Variable	Unit	Value
Modulus of Elasticity	E	GPa	8
Flexural Strength	σ_f	kPa	500
Poisson Ratio	ν	-	0.3
Ice Density	ρ_I	kgm^{-3}	910
Water Density	ρ_W	kgm^{-3}	1025
Gravity	g	ms^{-2}	9.81

$$Fr_I = \frac{v_S}{\sqrt{gH\eta}} \tag{20}$$

where C_p is the coefficient of ice resistance, η is the ice concentration, and Fr_I is the ice Froude number. It is considered that $n = 2$ based on Molyneux & Kim [26]. Furthermore, $k_b = 0.8267$ and $k_c = 4.4$ based on Chun-yu et al [27].

The various parameters for ice used in the described equations are summarized in Table 4.

3.4 Route and Voyages

The case study is performed on voyages between Kiel, Germany and Lulea, Sweden, including ice conditions in the Baltic sea, in weak or extremely weak ice winter [28]. Three voyage conditions are considered: (i) Summer voyage, (ii) Winter voyage without ice, and (iii) Winter voyage with ice. The ice concentration and ice thickness during a mild Baltic winter over the selected route are shown in Figure 5. The vessel travels nominally at a speed of 10 kn in open water and slows down in ice if the required power exceeds the installed power, while maintaining a minimum speed of 3 kn.

4. RESULTS AND DISCUSSION

4.1 Load profiles over simulated voyages

The propulsion powers are determined for the three voyage conditions using the methodology described in Section 2.1, applied over the route and environmental conditions described in Section 3.4. Hotelling power demands are considered to be constant at 200 kW for a summer voyage, and 300 kW for a winter voyage. The resulting time-based propulsion and total power demand for all three voyages are shown in Figure 6.

The propulsion load stays at nearly constant load levels in the absence of level ice in both winter and summer. The summer propulsion demands averages around 218 kW with a standard deviation of 5 kW, for a voyage at 10 kn. Accordingly, the total power demand averages around 418 kW with a similar standard deviation. The average propulsion power demand in winter in the absence of level ice is 261 kW with a standard deviation of 40 kW, at 10 kn. The average total power demand is therefore 561 kW. The voyage involving level ice shows two distinct load levels, with the lower load level corresponding to the voyage before the vessel reaches the level ice at 10 kn. The propulsion load and the total power demand in level ice are limited at 950 kW and 1250 kW, respectively, by slowing the vessel down to 3 kn during this time. The power requirements over the simulated voyages can be met by the determined onboard installed power.

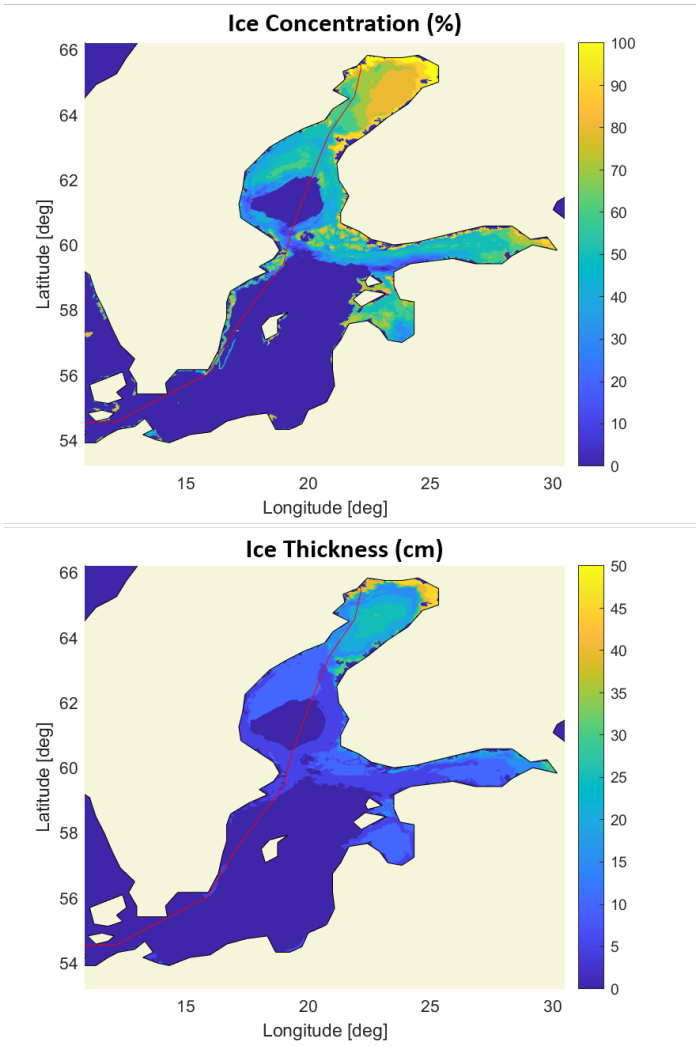

FIGURE 5: ROUTE, ICE CONCENTRATION [%], ICE THICKNESS [CM]

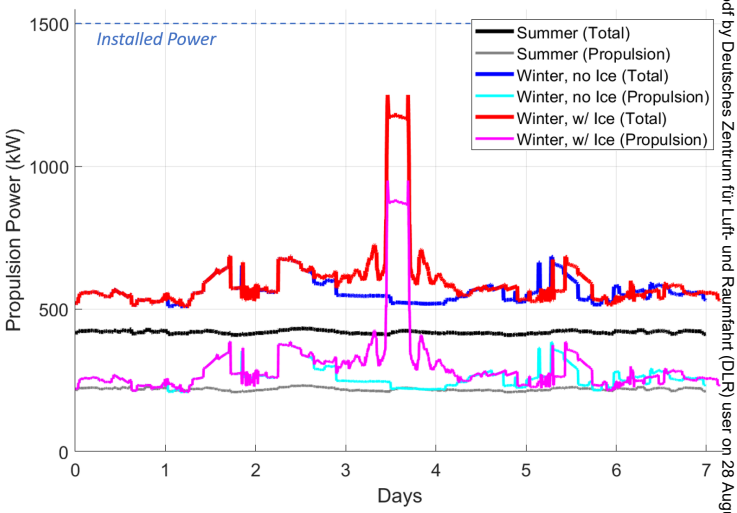

FIGURE 6: LOAD PROFILES OVER THE THREE VOYAGES

4.2 Impact of component sizing on energy efficiency

The developed energy system models and energy management algorithm are implemented to determine the optimal fuel energy consumption of a given energy system configuration over the various defined voyages. Various component sizing parameters such as (a) rated power of gensets, (b) number of installed gensets, and (c) battery capacity are simulated, to assess the impact of these parameters on overall energy efficiency. The various fixed and varying parameters simulated are summarized in Table 5.

The total installed diesel genset power onboard is maintained constant at 1500 kW. Different genset configurations are simulated, ranging from installing a single genset rated at 1500 kW to installing five smaller gensets, each rated at 300 kW. The battery capacity is varied between 0 kWh (no battery present) and 500 kWh for each genset configuration. The battery is assumed to have a 2C-rating, resulting in up to 1 MW of charging or discharging power from the battery. However, the battery power is not included in the calculation of the total installed power. Finally, a minimum operating power reserve ('spinning reserve') of 75 kW is maintained at all times, to enable power response to rapid transient load demands and enable maneuverability of the vessel.

TABLE 5: ENERGY SYSTEM PARAMETERS SIMULATED

Parameter	Variable	Value / Sweep Range
Total Genset Capacity	P_g^{max}	1500 kW
Number of Gensets	N_g^{max}	1 ... 5 (5 steps)
Battery Capacity	E_b^{max}	0 ... 500 kWh (6 steps)
Battery Power Rating	P_b^{max}	$2E_b^{max}$
Power Reserve Coeff	ΛP_g^{max}	75 kW
Voyages		Summer, Winter (no ice), Winter (with ice)

Figure 7 shows the variation in fuel consumption for different numbers of installed gensets while maintaining the total installed power constant at 1500 kW, for different battery sizes, over all three considered voyages. Installing a greater number of smaller gensets results in 13.8%, 7.8%, and 6.9% energy savings over an energy system consisting of a single genset, over the summer, winter (without ice), and winter (with ice) voyages, respectively. Most of the vessel operation occurs at low loads, as the ice-class energy system is over-dimensioned for typical voyages without ice. A single genset therefore operates at low loads corresponding to low efficiencies, while an energy system with multiple smaller gensets can operate more efficiently with fewer gensets operating at higher loads. However, the variation of fuel energy with increasing genset modularity is not monotonic, as 3- and 5- gensets show slightly higher energy consumption than 2- and 4- gensets, respectively, over the winter voyages. However, the summer voyage is more efficient with 3 gensets installed than with 4 gensets.

The trends can be explained by Figure 8, which shows the histogram of genset power and time-series data of number of active gensets, for the points (a), (b) and (c) marked in Figure 7. A

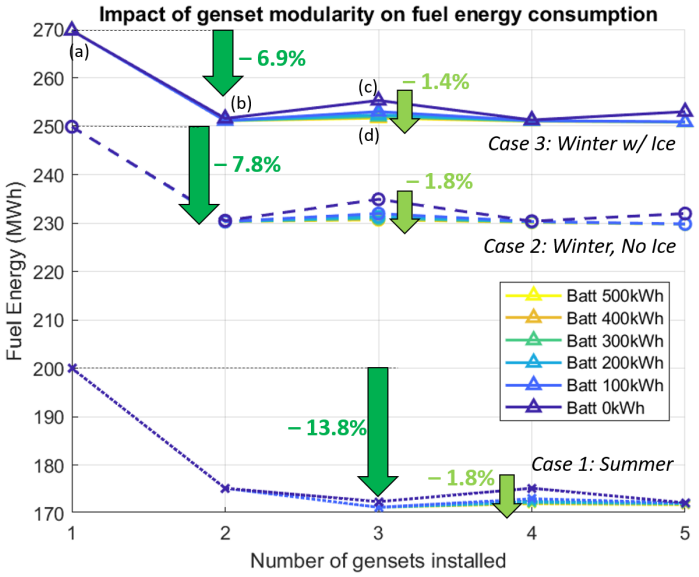

FIGURE 7: VARIATION OF FUEL ENERGY CONSUMED FOR DIFFERENT GENSET MODULARITY AND BATTERY SIZES, OVER ALL THREE VOYAGE CONDITIONS

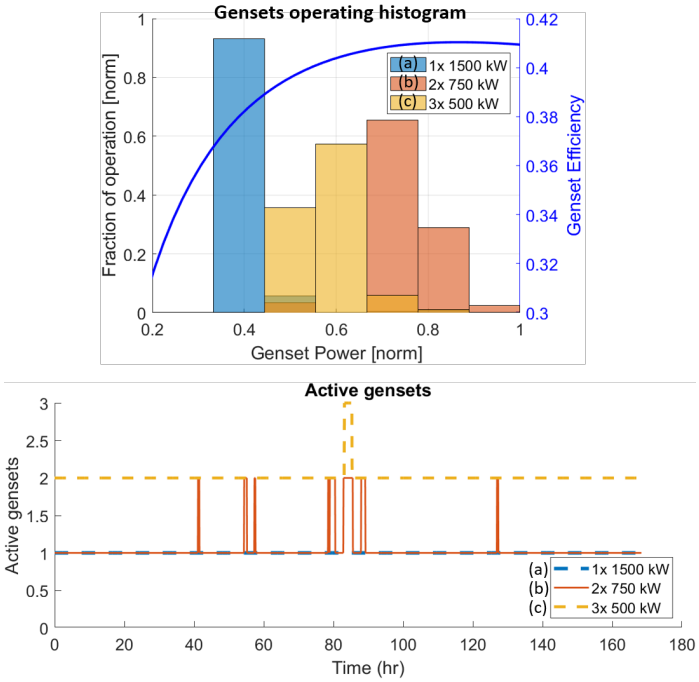

FIGURE 8: IMPACT OF INSTALLING MULTIPLE SMALLER GENSETS OVER A WINTER VOYAGE WITH ICE

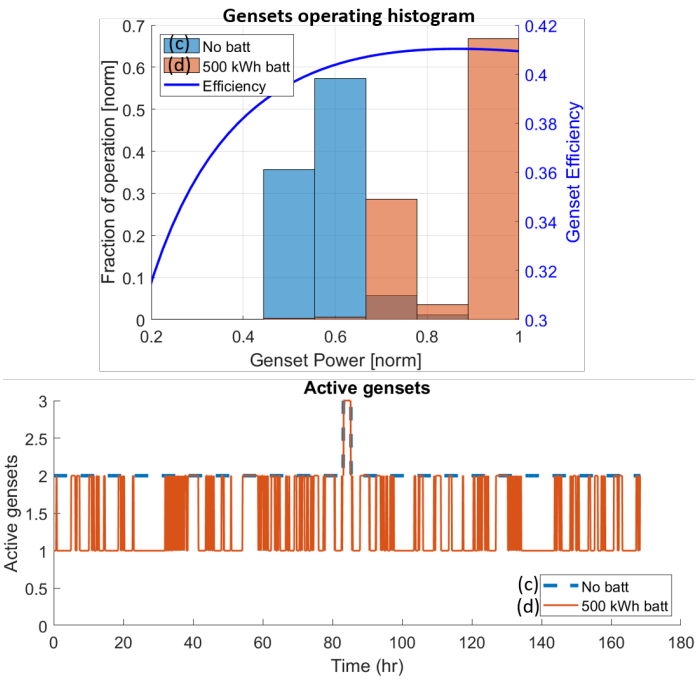

FIGURE 9: IMPACT OF HYBRIDIZING AN ENERGY SYSTEM CONSISTING OF THREE DIESEL GENSETS WITH A 500 KWH BATTERY, OVER A WINTER VOYAGE WITH ICE

single genset rated at 1500 kW operates mostly around 40% of its peak power over the winter voyage with ice. When two gensets of 750 kW rating are installed, most of the load demands can be met by a single genset operating at 70%-90% of its rated power where the efficiencies are higher. The second genset is turned ON only when power demands are high, which occur relatively rarely in the simulated voyages. However, an energy system comprising of three 500 kW gensets needs to operate with two active gensets, each operating around 40%-70% of the rated power, where efficiencies are lower than case (b). Therefore, it can be concluded that increasing modularity does not guarantee energy savings, and strongly depends on the power levels demanded from the voyage.

It is also observed in Figure 7 that battery hybridization does not impact energy efficiency for most scenarios, while 1.4%-1.8% energy savings are observed for specific genset modularities. The battery eliminates the inefficiencies when the genset modularity is not optimal for a specific voyage, by enabling the gensets to operate at higher efficiencies and accounting for the difference in power. This is confirmed by Figure 9, which shows the genset operating histogram and time-series of number of active gensets for scenarios (c) and (d) marked in Figure 7. The presence of a battery enables intermittent operation of two and three gensets, such that the active gensets operate at higher loads and therefore higher efficiencies. The battery accordingly charges or discharges to account for the power difference. Therefore, it can be concluded that although batteries do not provide outright fuel efficiency benefits over the simulated voyages, they robustly enable optimal operation over different load profiles.

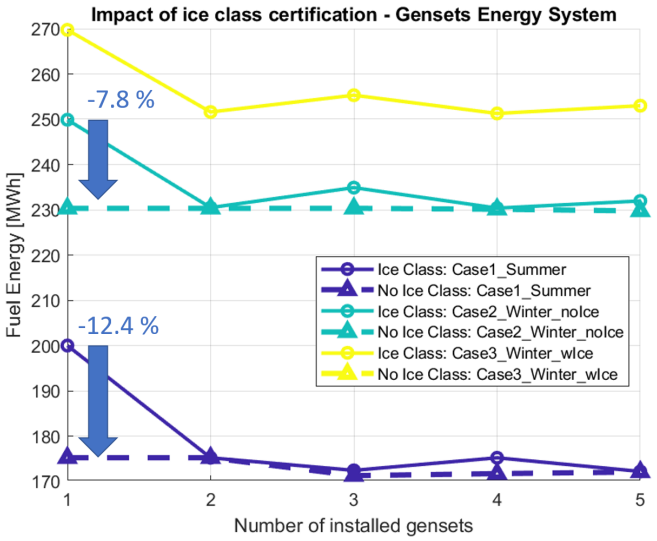

FIGURE 10: VARIATION OF FUEL ENERGY CONSUMED FOR DIFFERENT GENSET MODULARITY WITH- AND WITHOUT- ICE CLASS CERTIFICATION, OVER ALL THREE VOYAGE CONDITIONS

4.3 Impact of ice class certification on energy efficiency

The energy system for an ice class vessel is typically oversized for summer and winter voyages in open water, as shown in Figure 6, as the peak load demand without level ice conditions does not exceed 700 kW. In this section, the impact of an ice class energy system on energy efficiency over summer and winter (no ice) voyages is investigated by comparing its performance against another, downsized, energy system with a peak installed power of 750 kW. A component sizing sweep is performed similar to that described in Section 4.1, wherein the number and sizes diesel gensets are varied without a battery.

Figure 10 compares the energy efficiency of an ice-class energy system (solid lines) with a downsized energy system (dashed lines) for two voyages, for a genset-only energy system involving one, two, and three gensets. A downsized energy system with only one genset results in 12.4% and 7.8% energy savings over the summer and winter (no ice) voyages, respectively. This is because the downsized genset operates closer to its rated power where efficiencies are higher. The genset operating histograms in Figure 11(a) confirm this trend, showing genset operation at higher powers and therefore higher efficiencies.

An ice class energy system comprising of two smaller gensets performs just as efficiently as a downsized energy system over both the voyages. One of the two smaller gensets in the ice-class energy system is turned OFF during low power demands in summer, making this system operation identical to that of a downsized energy system, as shown in Figure 11(b). The energy efficiency of the ice class vessel with three smaller gensets slightly improves over the summer voyage and deteriorates over the winter voyage. This is because the winter power profiles require the operation of two gensets at lower efficiency, while the summer power can be delivered by a single genset at higher efficiency, as shown in Figure 11(c).

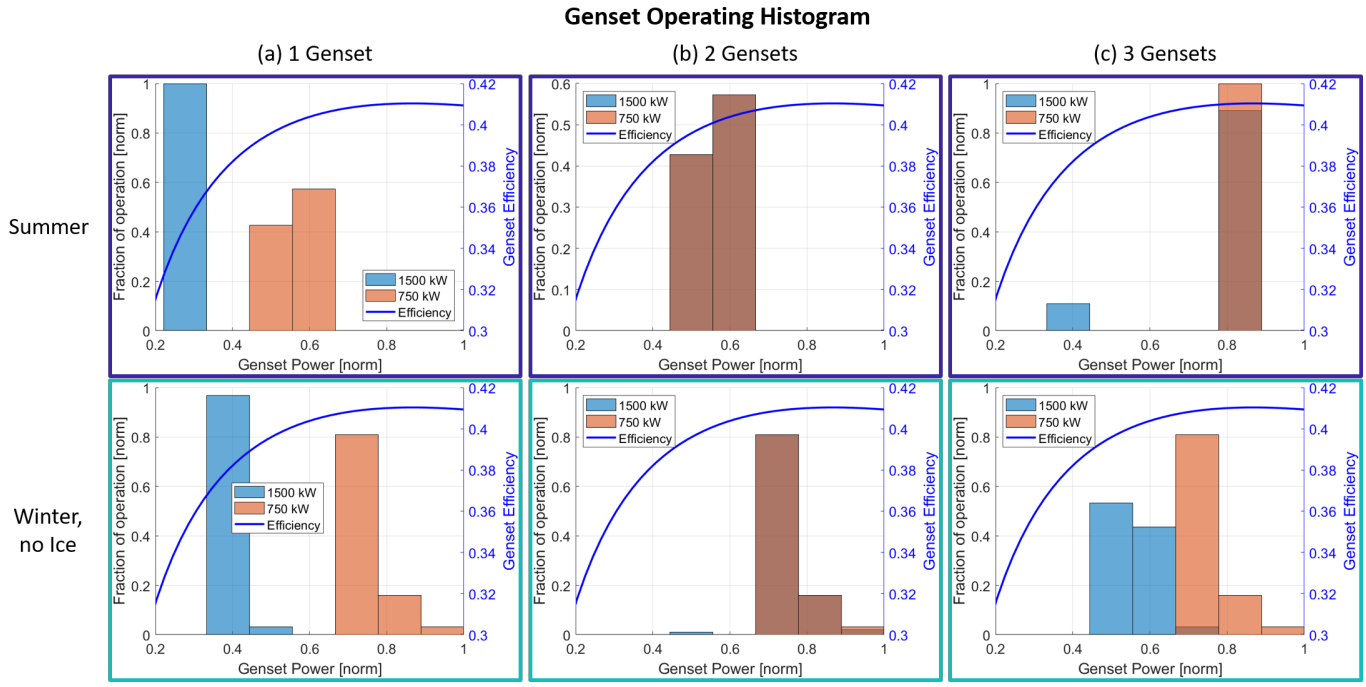

FIGURE 11: ENGINE OPERATING HISTOGRAMS FOR SCENARIOS WITH- AND WITHOUT- ICE CLASS CERTIFICATION FOR DIFFERENT GENSET MODULARITY DURING SUMMER AND WINTER (NO ICE) VOYAGE CONDITIONS

5. SUMMARY AND CONCLUSION

This paper analyzes the performance of a hybrid energy system consisting of diesel gensets and a battery on an ice-class research vessel. First, the vessel power demand is calculated in open water, level ice and broken ice conditions. The weather and ice conditions over a selected route are obtained from the Copernicus database, and the time-varying propulsion power demand is calculated over the route. An optimization-based energy management algorithm based on simplified energy system models is implemented to achieve the optimal fuel energy consumption over the load profile. The developed approaches are implemented for a case study involving a research vessel travelling between Kiel, Germany and Lulea, Sweden. Three voyage conditions are simulated: (i) summer, (ii) winter, and (iii) winter with level ice present, for different hybrid energy system configurations. The following conclusions are valid based on the presented approach.

The peak propulsion load over a winter voyage with level ice, even for weak/mild Baltic winters can be up to 4.1 times higher than the peak propulsion load in summer. Modularizing the diesel genset installation by using multiple, smaller units can yield up to 13.8% energy savings, however, high modularity does not always guarantee better performance. Battery hybridization does not result in energy savings over most of the simulated cases, however, it compensates for non-optimal genset modularity over specific scenarios by yielding up to 1.8% fuel savings, thereby enabling optimal energy system operation over a wider range of voyages. Finally, it is shown that an ice class certified energy system performs just as efficiently as a comparable downsized energy system, if the genset installation is appropriately modularized.

ACKNOWLEDGMENTS

Part of this work has received funding from European Union's HORIZON research and innovation programme under the Grant Agreement no. 101138583 (MISSION project https://missionproject.eu/)

REFERENCES

[1] Silber, Gregory K. and Adams, Jeffrey D. "Vessel Operations in the Arctic, 2015–2017." *Frontiers in Marine Science* Vol. 6 (2019). DOI 10.3389/fmars.2019.00573.

[2] Heikkilä, Mikko, Grönholm, Tiia, Majamäki, Elisa and Jalkanen, Jukka-Pekka. "Effect of ice class to vessel fuel consumption based on real-life MRV data." *Transport Policy* Vol. 148 (2024): pp. 168–180. DOI https://doi.org/10.1016/j.tranpol.2024.01.014.

[3] Braithwaite, RC and Khan, D. "Implications of ice class for an offshore patrol vessel." *Journal of Marine Engineering & Technology* Vol. 13 No. 3 (2014): pp. 17–27. DOI 10.1080/20464177.2014.11658118.

[4] Tomi Solakivi, Tuomas Kiiski and Ojala, Lauri. "The impact of ice class on the economics of wet and dry bulk shipping in the Arctic waters." *Maritime Policy & Management* Vol. 45 No. 4 (2018): pp. 530–542. DOI 10.1080/03088839.2018.1443226.

[5] Wang, Zhuang, Chen, Li, Guo, Fengxiang and Wang, Bin. "Optimal Design of Hybrid Electric Propulsive System for A Mini Polar Cruise.": pp. ISOPE–I–21–1274. 2021.

[6] Zhou, Yi, Pazouki, Kayvan and Norman, Rose. "The Modelling and Optimal Control of a Hybrid Propulsion System for an Ice-Capable Ship." Vol. Volume 7A: Ocean Engineer-

ing: p. V07AT06A031. 2019. DOI 10.1115/OMAE2019-95142.

[7] Zhou, Yi, Pazouki, Kayvan and Norman, Rose. "The modelling and three-level control of a hybrid propulsion system for a green ice-capable ship." *Journal of Cleaner Production* Vol. 296 (2021): p. 126577. DOI https://doi.org/10.1016/j.jclepro.2021.126577.

[8] Hanninen, Samuli, Viherialehto, Sampo, Heideman, Torsten, Maattanen, Pirjo and Arslan, Ahmad. "Results From The World's Largest Arctic Ships and Advancements of Propulsion Technology." Vol. Day 1 Wed, March 08, 2023: p. D011S001R001. 2023. DOI 10.5957/TOS-2023-011.

[9] Hanninen, Samuli, Hakala, Jani, Viherialehto, Sampo, Maattanen, Pirjo and Heideman, Torsten. "Introduction of Azipod DI and ESS for Icebreakers." Vol. Day 3 Wed, May 03, 2023: p. D031S111R001. 2023. DOI 10.4043/32491-MS.

[10] Fengxiang, Guo, Li, Chen and Wenlong, Du. "Bi-objective optimization of diesel/battery hybrid electric propulsion system for polar icebreaker." Vol. All Days: pp. ISOPE–I–21–1275. 2021.

[11] Zhu, Jianyun, Chen, Li, Wang, Bin and Liu, Qiang. "A Multi-Objective Optimization Method for Hybrid Electric Propulsion System.": pp. ISOPE–I–18–176. 2018. URL https://onepetro.org/ISOPEIOPEC/proceedings-pdf/ISOPE18/All-ISOPE18/ISOPE-I-18-176/1196237/isope-i-18-176.pdf.

[12] Kondratenko, Aleksander A., Bergström, Martin, Reutskii, Aleksander and Kujala, Pentti. "A Holistic Multi-Objective Design Optimization Approach for Arctic Offshore Supply Vessels." *Sustainability* Vol. 13 No. 10 (2021). DOI 10.3390/su13105550.

[13] Kondratenko, Aleksander A., Kujala, Pentti and Hirdaris, Spyros E. "Holistic and sustainable design optimization of Arctic ships." *Ocean Engineering* Vol. 275 (2023): p. 114095. DOI https://doi.org/10.1016/j.oceaneng.2023.114095.

[14] Palmén, Mikael, Lotrič, Ajda, Laakso, Aleksi, Bolbot, Victor, Elg, Mia and Valdez Banda, Osiris A. "Selecting Appropriate Energy Source Options for an Arctic Research Ship." *Journal of Marine Science and Engineering* Vol. 11 No. 12 (2023). DOI 10.3390/jmse11122337.

[15] Fitz, Annika, Gosala, Dheeraj, Gosala, Vaidehi, Lampe, Tobias, Stutz, Sophie, Schwedt, Thorben and Ehlers, Sören. "Odyssa - A techno-economic evaluation framework for wind-assisted vessels with hydrogeneration." *Ships and Offshore Structures* Vol. TBC (2025). DOI TBC.

[16] Gosala, Dheeraj. "Convex Optimization-based Energy Management of an All-Electric Hybrid Ship." *TBD* Vol. TBD (TBD). DOI TBD.

[17] Holtrop, J. and Mennen, G.G.J. "An approximate power prediction method." *International Shipbuilding Progress* Vol. 29 No. 335 (1982). DOI 10.3233/ISP-1982-2933501.

[18] Chakrabarti, S.K. *Handbook of Offshore Engineering*. Elsevier (2005).

[19] (ITTC), International Towing Tank Conference. *Recommended Procedures and Guidelines: Preparation, Conduct and Analysis of Speed and Power Trials* (2022). URL https://ittc.info/media/10174/75-04-01-011-2022.pdf.

[20] Blendermann, W. "Parameter identification of wind loads on ships." *Journal of Wind Engineering and Industrial Aerodynamics* Vol. 51 (1994). DOI https://doi.org/10.1016/0167-6105(94)90067-1.

[21] Copernicus Marine Service. "Copernicus My Ocean Pro." https://data.marine.copernicus.eu/viewer. Accessed: 2024-12-13.

[22] Elbert, Philipp, Nuesch, Tobias, Ritter, Andreas, Murgovski, Nikolce and Guzzella, Lino. "Engine On/Off Control for the Energy Management of a Serial Hybrid Electric Bus via Convex Optimization." *IEEE Transactions on Vehicular Technology* Vol. 63 No. 8 (2014): pp. 3549–3559.

[23] *THE STRUCTURAL DESIGN AND ENGINE OUTPUT REQUIRED OF SHIPS FOR NAVIGATION IN ICE - FINNISH-SWEDISH ICE CLASS RULES* (2017). URL https://www.sjofartsverket.se/globalassets/isbrytning/pdf-regelverk/finnish-swedish_iceclass_rules.pdf.

[24] Lindqvist, G. "A straightforward method for calculation of ice resistance of ships." *Proceedings of the 10th International Conference on Port and Ocean Engineering under Arctic Conditioons POAC'89*. 1989.

[25] Xue, Y., Zhong, K., Ni, B.Y., Li, Z., Bergström, M., Ringsberg, J.W. and Huang, L. "A combined experimental and numerical approach to predict ship resistance and power demand in broken ice." *Ocean Engineering* Vol. 292 (2024). DOI https://doi.org/10.1016/j.oceaneng.2023.116476.

[26] Molyneux, K.M. and Kim, H.S. "Model Experiments to support the design of larged icebreaking tankers." *Proceedings of Design and Construction of Vessels Operating in Low Temperature Environments, National Research Councic Canada*. 2007.

[27] Chun-yu, G., Xie, C., Zhang, J.Z., Wang, S. and Zhao, D.G. "Experimental Investigation of the Resistance Performance and Heave and Pitch Motions of Ice-Going Container Ship Under Pack Ice Conditions." *China Ocean Engineering* Vol. 32 (2018). DOI 10.1007/s13344-018-0018-9.

[28] Aldenhoff, Wiebke. *The ice winter 2022/2023 at the German coasts and the Baltic Sea*. Bundesamt für Seeschiffahrt und Hydrographie (2024). URL https://www.bsis-ice.de/Eiswinter2023/HTML/Eiswinter2023en.html.

[29] Wang, Zhuang, Chen, Li, Zhou, Yinzheng, Guo, Nanhong and Wang, Bin. "Adaptive ECMS for Hybrid Power System of Mini Polar Cruise Ship." Vol. All Days: pp. ISOPE–I–22–348. 2022.

[30] Young Rong, K., Ehsan, E. and Sverre, S. "A meta-model for added resistance in waves." *Ocean Engineering* Vol. 266 (2022). DOI https://doi.org/10.1016/j.oceaneng.2022.112749.